

Brazing Inconel 625 for Plate Heat Exchanger

Wen-Shiang Chen ¹⁾ and *Ren-Kae Shiue²⁾

^{1,2)} *Department of Materials Science and Engineering, National Taiwan University,
Taipei 106, Taiwan*

²⁾ rkshiue@ntu.edu.tw

ABSTRACT

The purpose of this research is developing plate heat exchanger for special applications. The technology of manufacturing plate heat exchangers is much more difficult than that of making traditional heat exchangers. The plate heat exchanger is currently made by Cu brazing for most major heat exchanger manufacturer in the world. Stable brazing process and inexpensive filler alloy are primary advantages of Cu brazing. However, requirements of increased corrosion resistance, avoiding Cu ion contamination, resisting to high temperature and pressure resulting from various users make the Cu brazed stainless steel plate heat exchanger fail to satisfy all applications. Two novel amorphous Ni/(Fe)-based fillers are successfully applied in brazing IN-625 plate heat exchangers, and significantly improve the corrosion resistance of Cu brazed stainless steel plate heat exchanger. It is valuable for industrial applications.

1. INTRODUCTION

Inconel 625 (IN-625) has a nominal composition of 61Ni-21.5Cr-2.5Fe-9Mo-3.6Nb in wt%, and it is featured with high corrosion resistance to pitting, especially for the presence of chloride ions (e.g., sea water). (Smith 1990) Ni-based fillers are excellent choices in brazing IN-625 applied in elevated temperatures and severely corrosive environments. (Olson 1990) Most Ni-based fillers are alloyed with Cr for improved corrosion resistance, and alloyed with B and/or Si as melting point depressant(s) (MPDs). However, excessive addition of B and/or Si into the Ni-based fillers may results in forming brittle intermetallic phase(s) in both interface and brazed joint. (Massalski 1990) Because amorphous foils are featured with uniform chemical composition, they are suitable to be applied as brazing fillers. Two modified Ni-based amorphous brazing foils, MBF-51 (76.3Ni-15Cr-7.3Si-1.4B in wt%) and VZ-2106 (44Ni-35Fe-11Cr-1.5Mo-1.0Cu-6.4Si-1.5B in wt%), are applied in brazing IN-625. Many Ni-based filler foils have been suffered from high cost of Ni content in recent years. One of alternatives in reducing the material cost of Ni-based filler is to replace partial Ni

¹⁾ Graduate Student

²⁾ Professor

content by Fe in brazing filler. VZ-2106 is a novel Ni/Fe-based amorphous foil. About half of the Ni content is replaced by Fe, a much cheaper ingredient in the braze alloy.

2. EXPERIMENTAL PROCEDURE

Base metals used in the experiment were IN-625 template with the dimension of 15 mm in length, 15 mm in width and 3 mm in thickness. All joined surfaces were ground by SiC papers up to grit 600 and ultrasonically cleaned in acetone prior to brazing. MBF-51 and VZ-2106 amorphous foils with the thickness of 40 μm were chosen as braze alloys. Liquidus temperatures of MBF-51 and VZ-2106 amorphous foils are 1399 K and 1427K, respectively. Furnace brazing was performed under the vacuum of 5×10^{-5} mbar. The heating rate was set at 0.33 K/s throughout the experiment. All specimens were preheated at 1273 K for 600 s prior to brazing in order to equilibrate the temperature profile of the specimen. Brazing conditions used in the experiment are listed in [Table 1](#).

Cross-sections of joints after brazing were cut by a low-speed diamond saw and subsequently examined by using a JEOL JSM 6510 scanning electron microscope (SEM). Quantitative chemical analyses of various phases in the joint were performed using the 8600SX electron probe microanalyzer (EPMA) equipped with the wavelength dispersive spectroscope (WDS). Its operation voltage was 15 kV, and the minimum spot size was set at 1 μm . Tensile tests of selected brazed joints were performed based on the ASTM E8 specification,

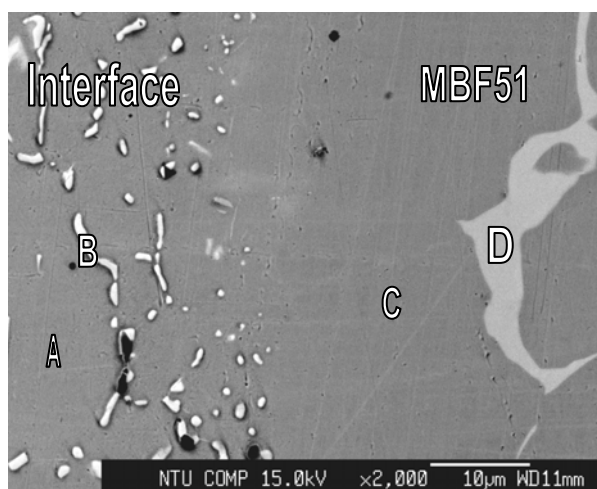
Table 1 Summary of brazing conditions used in the experiment

Filler Metal (wt%)	Brazing Temperature (K)	Brazing Time (s)	Thickness of Braze (μm)
MBF-51 (76.3Ni-15Cr-7.3Si-1.4B)	1423, 1453, 1473	600, 1800, 3600	40
VZ-2106 (44Ni-35Fe-11Cr-1.5Mo- 1.0Cu-6.4Si-1.5B)	1423, 1453, 1473	600, 1800, 3600	40

3. RESULTS AND DISCUSSION

[Figure 1](#) displays EPMA BEI and WDS chemical analysis results in atomic percent of IN-625/MBF-51/IN-625 joints brazed at 1453 K for 1800 s. There are two phases in the brazed joint, including Ni/Cr-rich matrix as marked by C and Nb/Ni/Si intermetallic compound as marked by D. According to the Nb-Ni-Si ternary alloy phase diagram, the stoichiometric ratio of Nb/Ni/Si intermetallic compound among Nb, Ni and Si is close to $\text{Nb}_6\text{Ni}_{16}\text{Si}_7$. ([Villars 1995](#)) $\text{Nb}_6\text{Ni}_{16}\text{Si}_7$ is a nonstoichiometric compound. Based on the WDS chemical analysis results, $\text{Nb}_6\text{Ni}_{16}\text{Si}_7$ is alloyed with Fe, Cr and Mo, so its composition is not exactly followed stoichiometrically. The formation of coarse $\text{Nb}_6\text{Ni}_{16}\text{Si}_7$ phase is resulted from solidification of molten braze during brazing. It is also

noted that grain boundary borides as marked by B and IN-625 matrix as marked by A are observed at the interface between MBF-51 braze and IN-625 substrate.



Element/Location	A	B	C	D
Fe	4.7	1.3	3.7	0.5
B	0.0	34.2	0.0	0.0
Si	0.1	0.0	1.1	22.7
Cr	25.8	20.5	24.7	4.1
Ni	62.5	10.0	64.6	54.4
Mo	4.4	28.4	3.9	2.9
Nb	2.1	5.3	1.7	15.4
Mn	0.4	0.2	0.3	0.0
Phase	Ni/Cr-rich (close to IN-625)	boride	Ni/Cr-rich matrix	$Nb_6Ni_{16}Si_7$

Fig. 1. EPMA BEI and WDS chemical analysis results in atomic percent of IN-625/MBF-51/ IN-625 joint brazed at 1453 K for 1800 s.

Figure 2 illustrates microstructural evolution of IN-625/MBF-51/IN-625 joints under various brazing conditions. Because dissolution of IN-625 substrate is not prominent at 1423 K, the amount of $Nb_6Ni_{16}Si_7$ phase is much less than that of specimens brazed at 1453 K. However, $Nb_6Ni_{16}Si_7$ is not a stable phase in the joint, and it is dissolved into the Ni/Cr-rich matrix at 1473 K. For the specimen brazed at 1473 K for 3600 s, $Nb_6Ni_{16}Si_7$ intermetallic compound disappeared from the joint, and only grain boundary borides are left behind the joint as illustrated in **Fig. 2(i)**. Increasing the brazing temperatures and/or time enhance the penetration depth of grain boundary borides. Higher brazing temperature and/or longer brazing time cannot remove grain boundary borides from the joint. On the contrary, grain boundary borides are coarsened with increasing the brazing temperature and/or time. **Figure 3** shows EPMA WDS chemical analysis depth profiles in at% across IN-625/MBF-51/IN-625 joint brazed at 1473 K for 3600 s. The WDS analyses were performed from center of the joint into IN-625 substrate with an interval of 8 μm for each analysis spot. The chemical composition of Ni/Cr-rich matrix is almost identical in both brazed joint and IN-625 substrate except for

slightly higher Si content in the brazed joint. It is consistent with chemical compositions of spot A and C shown in Fig. 1.

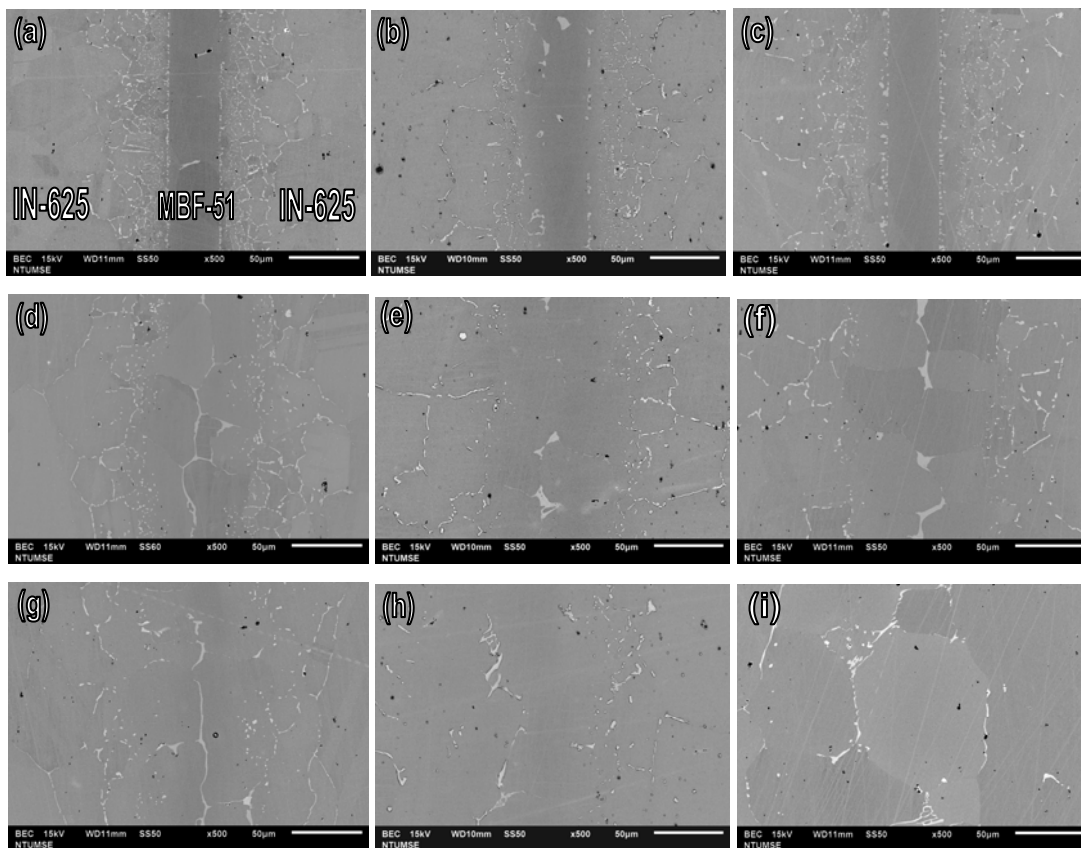


Fig. 2. EPMA BEIs of IN-625/MBF-51/IN-625 joints brazed at (a) 1423 K for 600 s, (b) 1423 K for 1800 s, (c) 1423 K for 3600 s, (d) 1453 K for 600 s, (e) 1453 K for 1800 s, (f) 1453 K for 3600 s, (g) 1473 K for 600 s, (h) 1473 K for 1800 s, (i) 1473 K for 3600 s.

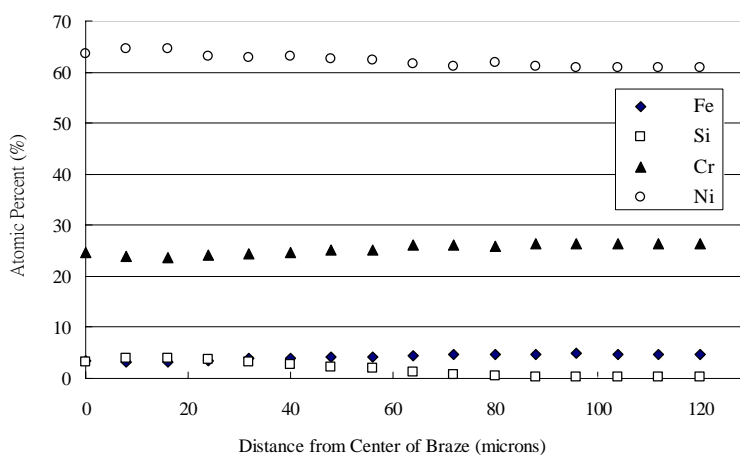
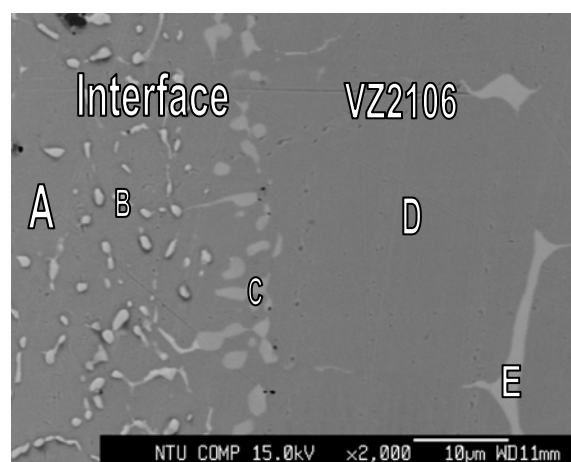


Fig. 3. EPMA WDS chemical analysis results in atomic percent across IN-625/MBF-51/IN-625 joint brazed at 1473 K for 3600s.

Figure 4 shows EPMA BEI and WDS chemical analysis results in atomic percent of IN-625/VZ-2106/IN-625 joint brazed at 1453 K for 1800 s. There are two major phases in the brazed joint, including Ni/Cr/Fe-rich matrix as marked by D and coarse $\text{Nb}_6\text{Ni}_{16}\text{Si}_7$ intermetallic compound as marked by E. The formation of coarse $\text{Nb}_6\text{Ni}_{16}\text{Si}_7$ with irregular shape is resulted from solidification of the molten melt. Different from the brazed IN-625/MBF-51/IN-625 joint, fine $\text{Nb}_6\text{Ni}_{16}\text{Si}_7$ precipitates as marked by C are observed at the interface between VZ-2106 braze and IN-625 substrate. Fine interfacial $\text{Nb}_6\text{Ni}_{16}\text{Si}_7$ precipitates are resulted from interfacial reaction between braze melt and IN-625 substrate. The Nb content in the $\text{Nb}_6\text{Ni}_{16}\text{Si}_7$ precipitate is originated from dissolution of IN-625 into the braze melt during brazing. It is obvious that the dissolution of IN-625 into VZ-2106 braze melt is less prominent than that into MBF-51 braze melt. The Si content of VZ-2106 braze tends to react with IN-625 substrate via solid state grain boundary diffusion of Si at the interface between VZ-2106 and IN-625. Similar to aforementioned result, the interface contains grain boundary boride as marked by B, and Ni/Cr-rich matrix as marked by A.



Element/Location	A	B	C	D	E
Fe	5.0	4.2	5.4	21.8	5.7
B	0.2	37.4	0.0	0.1	0.0
Si	0.4	0.4	20.4	5.6	23.4
Cr	25.8	18.5	5.8	17.5	3.4
Ni	61.9	20.3	51.8	51.7	49.3
Mo	4.2	16.0	2.5	2.1	3.7
Cu	0.1	0.1	0.1	0.4	0.1
Nb	2.1	3.1	13.8	0.6	14.4
Mn	0.4	0.1	0.1	0.2	0.1
Phase	Ni/Cr-rich (close to IN-625)	boride	$\text{Nb}_6\text{Ni}_{16}\text{Si}_7$	Ni/Cr/Fe- rich matrix	$\text{Nb}_6\text{Ni}_{16}\text{Si}_7$

Fig. 4. EPMA BEI and WDS chemical analysis results in atomic percent of IN-625/VZ-2106/ IN-625 joint brazed at 1453 K for 1800 s.

Figure 5 illustrates microstructural evolution of IN-625/VZ-2106/IN-625 joints under various brazing conditions. The amount of central coarse $\text{Nb}_6\text{Ni}_{16}\text{Si}_7$ phase in Fig. 5 is less than that in Fig. 2 due to the presence of grain boundary $\text{Nb}_6\text{Ni}_{16}\text{Si}_7$ phase. It indicates that dissolution of IN-625 substrate into VZ-2106 melt is less prominent than that into MBF-51 melt. Accordingly, the effect of substrate erosion into the VZ-2106 melt during brazing is not prominent in brazing IN-625. The depletion of $\text{Nb}_6\text{Ni}_{16}\text{Si}_7$ phase from the braze alloy into interface primarily via grain boundary diffusion are demonstrated in the figure. Additionally, grain boundary borides are coarsened with increasing the brazing temperature and/or time, especially for the specimen brazed at 1473 K for 3600 s as illustrated in Fig. 5(i). The coarsening of grain boundary borides at the interface between VZ-2106 and IN-625 substrate results in disappearance of fine grain boundary borides. The vanish of fine grain boundary borides in brazing IN-625 using the Ni/Fe-based filler metal, VZ-2106, is very different from that in brazing stainless steel using traditional Ni-based fillers. For example, the martensitic stainless steel brazed with Ni-based filler foil, continuous grain boundary boride(s) cannot be removed from the joint even for extended brazing temperature and/or time.

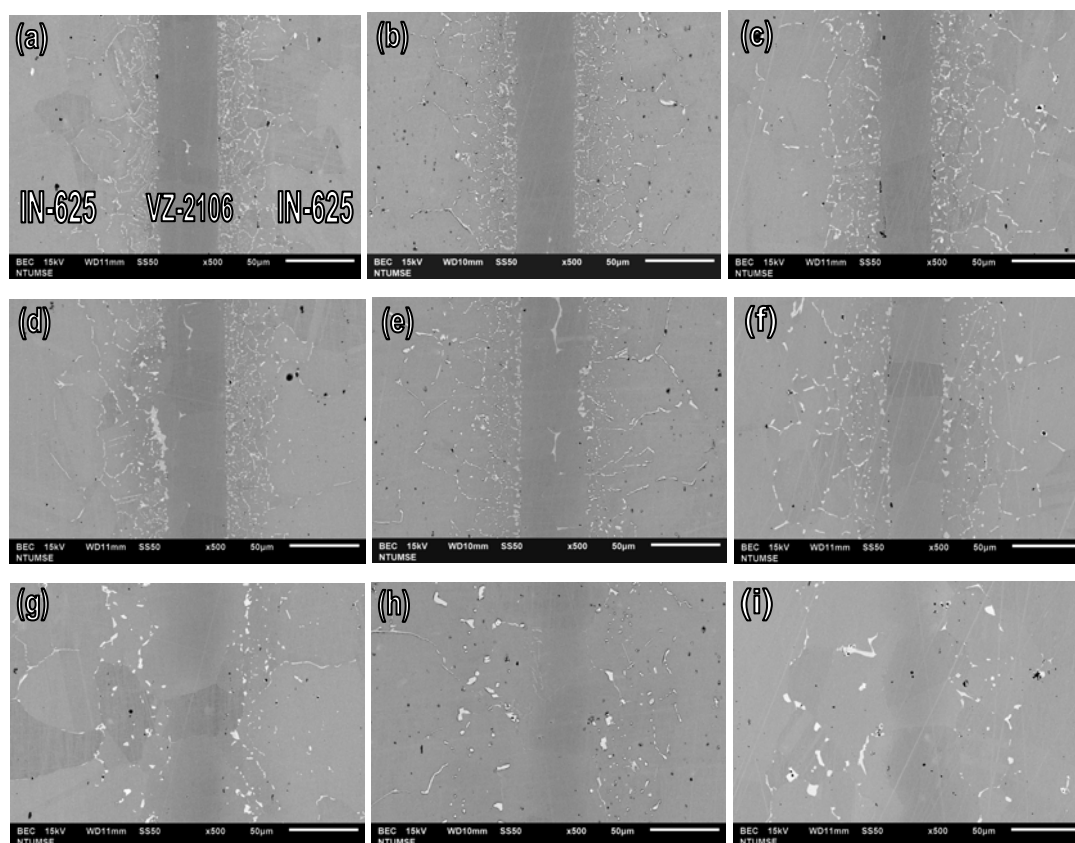


Fig. 5 EPMA BEIs of IN-625/VZ-2106/IN-625 joints brazed at (a) 1423 K for 600 s, (b) 1423 K for 1800 s, (c) 1423 K for 3600 s, (d) 1453 K for 600 s, (e) 1453 K for 1800 s, (f) 1453 K for 3600 s, (g) 1473 K for 600 s, (h) 1473 K for 1800 s, (i) 1473 K for 3600 s.

Figure 6 shows EPMA WDS chemical analysis depth profiles in at% across IN-625/VZ-2106/IN-625 joint brazed at 1473 K for 3600 s. The WDS analyses were performed from center of the joint into IN-625 substrate with an interval of 8 μm for each analysis spot. Different from the aforementioned result, central Ni/Cr/Fe-rich matrix in the brazed joint is gradually changed into Ni/Cr-rich matrix in the IN-625 substrate. It is consistent with chemical compositions of spot A and D shown in Fig. 4.

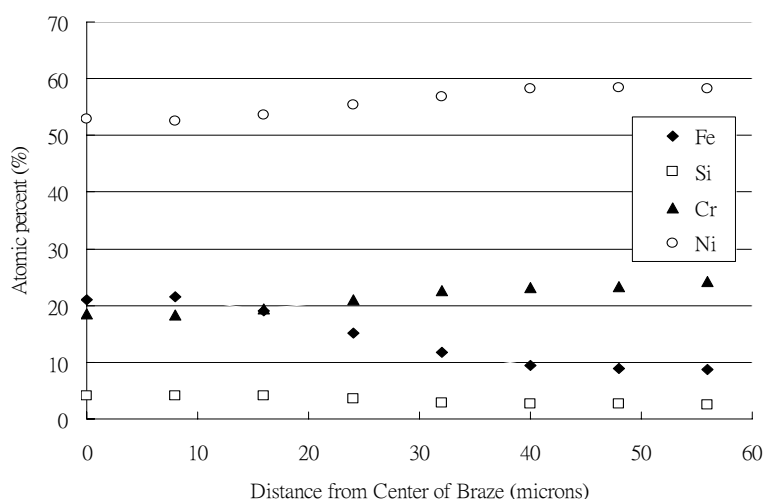


Fig. 6. EPMA WDS chemical analysis results in atomic percent across IN-625/VZ-2106/IN-625 joint brazed at 1473 K for 3600 s.

Table 2 Tensile strengths of selected brazed joints

Filler Metal	Brazing Temperature / Time (K / s)	Tensile Strength (MPa)
MBF-51	1453 / 1800	443 ± 15
	1473 / 1800	317 ± 10
VZ-2106	1453 / 1800	309 ± 12
	1473 / 1800	293 ± 9

Strengths of amorphous MBF-51 and VZ-2106 foils are not related to those of brazed joints, since the amorphous brazing foils are crystallized after brazing. Strengths of crystallized joints depend on microstructure and phase(s) of the joint. Table 2 displays tensile strengths of selected brazed joints. For the MBF-51 filler, the joint brazed at 1453 K for 1800 s has the maximum tensile strength of 443 MPa, and increasing brazing temperature results in decreasing bonding strength of the joint. In contrast, brazed joints using VZ-2106 filler have ultimate tensile strength of approximately 300 MPa. Both IN-625 substrate and the interface between the braze and IN-625 are not failed. All specimens are fractured at the brazed zone, which is dominated by Ni/Cr/(Fe)-rich matrix. Because the presence of fine grain boundary

borides is not continuous, they show little effect on tensile strengths of brazed joints in the experiment. Quasi-cleavage and transgranular fracture are widely observed from all fractured surfaces. For the MBF-51 filler foil, higher brazing temperature results in lower tensile strength of the joint due to coarser Ni/Cr-rich matrix grains. For the VZ-2106 filler foil, similar fractographs are observed from both brazing temperatures. Quasi-cleavage and transgranular fracture of Ni/Cr/Fe-rich matrix are observed from the VZ-2106 brazed joints.

4. CONCLUSION

Brazing IN-625 substrate using MBF-51 and VZ-2106 amorphous filler foils has been investigated in the study. The brazed joint primarily consists of interfacial grain boundary borides, coarse $Nb_6Ni_{16}Si_7$ and Ni/Cr/(Fe)-rich matrix. Higher brazing temperature and/or longer brazing time result in disappearance of coarse $Nb_6Ni_{16}Si_7$ intermetallic compound, and fine grain boundary borides are replaced by isolated coarse borides in Ni/Cr/(Fe)-rich matrix. For MBF-51 filler, maximum tensile strength of 443 MPa is obtained from the specimen brazed at 1453 K for 600 s. In contrast, tensile strengths of VZ-2106 brazed IN-625 specimens are approximately 300 MPa. All fractographs are featured with quasi-cleavage fracture. Both amorphous filler foils demonstrate potential in brazing IN-625 substrate for industrial application.

ACKNOWLEDGEMENTS

Authors gratefully acknowledge the financial support of this research by National Science Council (NSC), Taiwan, Republic of China, under grant number NSC 99-2221-E-002-120- MY3.

REFERENCES

- Massalski, T.B. (1990). *Binary Alloy Phase Diagrams*, ASM International, Materials Park.
- Olson, D.L. (1990). *Metals Handbook, Vol. 6 Welding Brazing and Soldering*, ASM International, Materials Park.
- Smith, W.F. (1993). *Structure and Properties of Engineering Alloys*, McGraw-Hill Inc., New York.
- Villars, P., Prince, A. and Okamoto, H. (1995). *Handbook of Ternary Alloy Phase Diagrams*, ASM International, Materials Park.